MOLECULAR AND CELLULAR BIOLOGY, Feb. 2011, p. 674–685 Vol. 31, No. 4
0270-7306/11/$12.00 doi:10.1128/MCB.01188-10

New Suppressors of THO Mutations Identify Thp3 (Ypr045c)-Csn12 as a Protein Complex Involved in Transcription Elongation▽†

Sonia Jimeno,[1] Cristina Tous,[1] María L. García-Rubio,[1,2] Michael Ranes,[1] Cristina González-Aguilera,[1,2] Antonio Marín,[2] and Andrés Aguilera[1,2]*

Centro Andaluz de Biología Molecular y Medicina Regenerativa (CABIMER), Av. Américo Vespucio s/n, 41092 Seville, Spain,[1] and Departamento de Genética, F. Biología, Universidad de Sevilla, Seville, Spain[2]

Received 8 October 2010/Returned for modification 16 November 2010/Accepted 3 December 2010

Formation of a ribonucleoprotein particle (mRNP) competent for export requires the coupling of transcription with mRNA processing and RNA export. A key link between these processes is provided by the THO complex. To progress in our understanding of this coupling, we have performed a search for suppressors of the transcription defect caused by the *hpr1*Δ mutation. This has permitted us to identify mutations in the genes for the RNA polymerase II mediator component Med10, the Sch9 protein kinase, and the Ypr045c protein. We report a role in transcription elongation for Ypr045c (Thp3) and the Csn12 component of the COP9 signalosome. Thp3 and Csn12 form a complex that is recruited to transcribed genes. Their mutations suppress the gene expression defects of THO complex mutants involved in mRNP biogenesis and export and show defects in mRNA accumulation. Transcription elongation impairment of *thp3*Δ mutants is shown by *in vivo* transcript run-on analysis performed in G-less systems. Thp3-Csn12 establishes a novel link between transcription and mRNA processing that opens new perspectives on our understanding of gene expression and reveals novel functions for a component of the COP9 signalosome. Thp3-Csn12 also copurifies with ribosomal proteins, which opens the possibility that it has other functions in addition to transcription.

Formation of a mature ribonucleoprotein particle (mRNP) competent for export requires the correct coupling of transcription with mRNA processing steps such as 5′-end capping, splicing, 3′-end cleavage, and polyadenylation, as well as with RNA export (1, 4, 9, 42). A connection between mRNP formation and transcription is provided by the conserved THO complex. In *Saccharomyces cerevisiae*, THO is composed of stoichiometric amounts of Tho2, Hpr1, Mft1, and Thp2 (7). It is recruited to active chromatin, functions during transcription elongation and RNA export, and physically associates with the RNA-dependent ATPase Sub2/UAP56 in a larger protein complex termed TREX (61). Different results reveal a functional relationship between THO and RNA export. These include the findings that mutations in RNA export factors such as Sub2, Yra1, the Mex67-Mtr2 heterodimer, or Nab2 hnRNP confer gene expression defects similar to those of THO mutants and that THO mutations confer synthetic lethality with RNA export mutations (35, 61). A hallmark of THO mutants is their strong genome instability phenotype that is linked to transcription elongation impairment and to the cotranscriptional formation of R loops (DNA-RNA hybrids) (2, 31).

The THSC complex, also termed TREX-2 (composed of Thp1, Sac3, Sus1, and Cdc31), is also involved in mRNP biogenesis and export, and the mutant forms of its components also confer gene expression and mRNA export defects and increased genome instability similar to those of THO mutants (19, 22, 24, 56, 68). Despite their similar phenotypes, in contrast to THO, which is found all over the nucleus, THSC is located primarily at the nuclear periphery in association with nucleoporins (19, 40). Notably, it has recently been shown that THSC physically interacts with Sem1 (15, 66), a factor that, in addition, interacts with other complexes such as the 19S proteasome (21) and the COP9 signalosome (CSN) (15). THSC, the proteasome, and the CSN all have among their components a subunit with a Sac3 domain and another subunit with a PAM domain (8, 15, 66).

The CSN was first identified in *Arabidopsis thaliana* as an eight-subunit complex involved in the suppression of light-dependent development (63). It is conserved from fission yeast to humans and is thought to be a regulator of signaling and developmental processes (20, 48, 65). The CSN is a multisubunit protease that regulates the activity of cullin-RING ligase families of ubiquitin E3 complexes via its deneddlyase activity. The conserved NEDD8 protein (Rub1 in *S. cerevisiae*) can be conjugated to substrate proteins in a process known as neddylation, a posttranslational protein modification closely related to ubiquitination. Neddylation is essential in most model organisms but not in *S. cerevisiae*, and it is reversed by NEDD8 isopeptidases such as yeast CSN5, a component of the CSN (see reference 54). In addition to its deneddylation function, it has also been shown that CSN influences the DNA damage response, cell cycle control, and gene expression, although the mechanism underlying these actions is unknown (6, 43). A CSN-like complex has been described in *S. cerevisiae* that it is composed of six subunits, Csn5, Csn9, Csn10, Csn11, Csn12, and Csi1 (46).

Despite the increasing data supporting the coupling between transcription and RNA export and its impact on genome instability, the function of the factors involved in this process is

* Corresponding author. Mailing address: Centro Andaluz de Biología Molecular y Medicina Regenerativa (CABIMER), Av. Américo Vespucio s/n, 41092 Seville, Spain. Phone: 34 954468372. Fax: 34 954461664. E-mail: aguilo@us.es.

† Supplemental material for this article may be found at http://mcb.asm.org/.

▽ Published ahead of print on 13 December 2010.

TABLE 1. Yeast strains used in this study

Strain	Genotype	Reference or source
AYW3-3C	*MATα ade2-1 can1-100 his3 ura3 leu2-k::ADE2-URA3::leu2-k hpr1ΔHIS3*	58
W303-1A	*MAT***a** *ade2-1 can1-100 his3-11 trp1-1 ura3-1 leu2-3,112*	R. Rothstein
WMK-1A	*MAT***a** *ade2-1 can1-100 his3-11 trp1-1 ura3-1 leu2-3,112 mft1ΔKAN*	7
U678-1C	*MAT***a** *ade2-1 can1-100 his3-11 trp1-1 ura3-1 leu2-3,112 hpr1ΔHIS3*	50
WSH-2A	*MATα ade2-1 can1-100 his3-11 trp1-1 ura3-1 leu2-3,112 hpr1Δ::HIS3 sem1ΔKAN*	This study
WMT-2C	*MAT***a** *ade2-1 can1-100 his3-11 trp1-1 ura3-1 leu2-3,112 yor045c-101 thp1Δ::KAN*	This study
BWCH-1B	*MAT***a** *his3 trp1 ura3 leu2 hpr1Δ::HIS3 csn12Δ::KAN*	This study
BWCS12-3B	*MAT***a** *ade2 his3 trp1 ura3 leu2 csn12Δ::KAN*	This study
WMM-12D	*MAT***a** *ade2-1 can1-100 his3-11 trp1-1 ura3-1 leu2-3,112 mex67-5 ypr045c-101*	This study
WSM-1D	*MAT***a** *ade2-1 can1-100 his3-11 trp1-1 ura3-1 leu2-3,112 ypr045c-101 sem1Δ::KAN*	This study
WWM-1D	*MAT***a** *ade2-1 can1-100 his3-11 trp1-1 ura3-1 leu2-3,112 ypr045c-101 mft1Δ::KAN*	This study
WM454-2B	*MATα ade2-1 can1-100 his3-11 trp1-1 ura3-1 leu2-3,112 ypr045c-101 GAL1p::YLR454w-TRP1*	This study
W303-454	*MAT***a** *ade2-1 can1-100 his3-11 trp1-1 ura3-1 leu2-3,112 GAL1p::YLR454w-TRP1*	45
WMC1	*MAT***a** *ade2-1 can1-100 his3-11 trp1-1 ura3-1 leu2-3,112 mex67-5*	35
WFBE046	*MAT***a** *ade2-1 can1-100 his3-11 trp1-1 ura3-1 leu2-3,112 thp1Δ::KAN*	22
BWC9H-1A	*MAT***a** *his3 trp1 ura3 leu2 csn9Δ::KAN hpr1Δ:HIS3*	This study
BWC9-4A	*MATα his3 trp1 ura3 leu2 csn9Δ::KAN*	This study
BWMN-2B	*MAT***a** *his3 trp1 ura3 leu2 ypr045cΔ::KAN*	This study
BWMH-8D	*MATα his3 trp1 ura3 leu2 ypr045cΔKAN hpr1ΔHIS3*	This study
BWMN-1A	*MAT***a** *ade2 his3 trp1 ura3 leu2*	This study
BWMN-1A	*MAT***a** *ade2 his3 trp1 ura3 leu2*	This study
WA41-2B	*MAT***a** *ade2-1 his3 ura3 leu2-k::ADE2-URA3::leu2-k hpr1Δ::HIS3 ypr045c-101*	This study
WA48-1D	*MATα ade2-1 his3 ura3 leu2-k::ADE2-URA3::leu2-k hpr1Δ::HIS3 med10-101*	This study
WB45-5B	*MAT***a** *ade2-1 can1-100 his3 ura3 leu2-k::ADE2-URA3::leu2-k hpr1Δ::HIS3 sch9-101*	This study
WA48-4B	*MATα ade2 his3 trp1 ura3 leu2-k::ADE2-URA3::leu2-k med10-101*	This study
WB45-1D	*MATα ade2 his3 trp1 ura3 leu-2k::ADE2-URA3::leu2-k sch9-101*	This study
WA41-1B	*MAT***a** *ade2 his3 trp1 ura3 leu2-k::ADE2-URA3::leu2-k hpr1ΔHIS3*	This study
WA41-6B	*MAT***a** *ade2 his3 trp1 ura3 leu2-k::ADE2-URA3::leu2-k*	This study
WCSHP-3B	*MAT***a** *ade2 his3 trp1 ura3 hpr1Δ::HIS3 csn12Δ::KAN*	This study
BWMN-2A	*MATα ade2 his3 trp1 ura3 hpr1Δ::HIS3*	This study
BWMN-3B	*MAT***a** *his3 trp1 ura3 hpr1Δ::HIS3 thp3Δ::KAN*	This study
Thp3-TAP	*THP3-TAP* integrated in BY4741	Open Biosystems
THTCS-9F	*CSN9-FLAG* integrated in the Thp3-TAP strain	This study
THTCS-12F	*CSN12-FLAG* integrated in the Thp3-TAP strain	This study
SYHPR1	*MAT***a** *ade2-1 can1-100 his3-11 trp1-1 ura3-1 leu2-3,112 HPR1-FLAG*	This study
SYTHP3	*MAT***a** *ade2-1 can1-100 his3-11 trp1-1 ura3-1 leu2-3,112 HPR1-FLAG thp3-101*	This study
BTHT-1D	*MAT***a** *ura3Δ0 his3 leu2Δ0 met-THP3-TAP::HIS3 thp1Δ::KAN*	This study
BTHH-6C	*MAT***a** *ura3 his3 leu2 met-THP3-TAP::HIS3 hpr1Δ::HIS*	This study

far from clear. To further understand this coupling, as mediated by the THO complex, we have performed a search for suppressors of the transcription defect of *hpr1*Δ that has permitted us to identify mutations in the gene of the RNA polymerase II (RNAPII) mediator component Med10, the Sch9 protein kinase, and the Ypr045c protein of unknown function. They suppress the transcription and RNA export defects, as well as the hyperrecombination phenotype, of THO mutants. A thorough analysis reveals that Ypr045c is recruited to transcribed chromatin and has a functional role in transcription elongation *in vivo*, even though an additional role in initiation cannot be excluded. We show that this novel protein, named Thp3, forms a physical and functional unit with the Csn12 component of the CSN and copurifies with ribosomal proteins. Our work establishes a new link between RNAPII transcription and a protein complex related to the CSN.

MATERIALS AND METHODS

Strains and plasmids. The yeast strains used in this study are listed in Table 1. Plasmid pCYC-LacZ was constructed by amplifying the *lacZ* gene from plasmid pCM184-LAUR with oligonucleotides LacZUp (5′AAGTACTCGAGACCATGATTACGGAT3′) and LacZ-Down (5′TCAGATCCGCGGTCGCTATGACG3′) using *Pfu* polymerase. A 2-kb fragment was cloned into pG-Leu-CYCds digested with XhoI after filling with Klenow fragment (C. Tous et al., unpublished data). Plasmids pG-Leu-CYCds (60), pCM184-LAUR and pCM184-LYΔNS (35), and pCM189-LEU2 (25) were previously described. For the amplification of the FLAG constructs, we used the pU6H10F plasmid (12).

Tn*3* insertion mutagenesis. Strain U678-1C was transformed with a yeast genomic library mutagenized by the insertion of an mTn*3*-*lacZ*/*LEU2* transposon (5). Sites of Tn*3* insertions were identified by the "vectorette" PCR rescue protocol (http://ygac.med.yale.edu/mtn/insertion_libraries.stm).

Chromatin immunoprecipitation (ChIP) analysis. For ChIP experiments, strains were grown either in rich medium (for *PMA1*) or in synthetic complete (SC) medium containing 2% glycerol and 2% lactate to an optical density at 600 nm (OD_{660}) of 0.5 (for *GAL1*). For *GAL1* ChIPs, the culture was split in two and one half was supplemented with 2% glucose (repressed transcription) and the other was supplemented with 2% galactose (activated transcription). Samples were then taken after 4 h of induction, and ChIP assays were performed as described previously (30). Anti-Rpb1-CTD monoclonal antibody 8WG16 (Berkeley Antibody Company) and protein A-Sepharose were used for RNAPII immunoprecipitation, and anti-FLAG M2 monoclonal antibody from Sigma was used for Hpr1-FLAG immunoprecipitation. Tandem affinity purification (TAP)-tagged versions of Thp3 and Csn12 were used. The GFX purification system (Amersham) was used for the last DNA purification step. We used the PCR of the intergenic region at positions 9716 to 9863 of chromosome V as a negative control. Real-time quantitative PCR and calculation of the relative abundance of each DNA fragment were performed as described previously (32). For each experiment, the DNA ratios in the different regions were calculated from the amount of DNA in these regions relative to that in the intergenic region. Medians and standard deviations (SD) of three independent experiments are shown.

***In vivo* G-less RNA-based run on (GLRO).** Strains harboring plasmid pG-Leu-CYCds or pCYC-LacZ were grown to an OD_{600} of 0.5 in SC medium lacking leucine (SC-leu) at 30°C. Run-on assays were carried out as previously described (60). Run-on products were digested with RNase T1, which cannot degrade G-less RNA, and resolved by 6% polyacrylamide gel electrophoresis (PAGE). Dried gels were analyzed with a phosphorimager (Fuji FLA-5100) using ImageQuant software (Molecular Dynamics). For each sample, the ratio of the total counts in the 132-nt G-less cassette band to those in the 262-nt G-less cassette band was determined (Tous et al., unpublished).

TAP-tagged purification of protein complexes. The Thp3-Csn12 complex was purified by using a TAP-tagged Thp3 protein (from Open Biosystems). The purification was essentially as described previously (55). The Thp3-TAP protein was isolated from yeast lysates by affinity purification using an IgG-Sepharose column. Proteins in the various elution fractions were concentrated with trichloroacetic acid, resolved by 8 to 16% gradient sodium dodecyl sulfate (SDS)-PAGE, and silver stained for visualization. Only the bands that did not appear in the negative control for the purification (nontagged strain) were used for matrix-assisted laser desorption ionization–time of flight (MALDI-TOF) mass spectrometry identification.

Coimmunoprecipitation analyses. For the coimmunoprecipitation studies, we integrated into the strain expressing the Thp3-TAP fusion protein either the Csn9-FLAG or the Csn12-FLAG fusion construct, which was obtained by PCR using primers CSN9-FW (5′-TCGGAGCTGGGAAACAAAGCTCAAACAGAATATATTGGAGtcccaccaccatcatcatcac-3′ [lowercase letters indicate the sequence corresponding to the FLAG epitope]) and CSN9-Rev (5′-CTAATATCGTCATTATTATGCCTTTTTCATATTTGATTTAactatagggagaccggcagatc-3′) or CSN12-FW (5′-CATCGTTTTCAGTAAGAAGGAGCCCTTTCCCCATAGCAAAtcccaccaccatcatcatcac3′) and CSN12-Rev (5′-TTTTTTTTTCTTCGTTCAATTATTGACTATTTTTCTATCAactatagggagaccggcagatc), using the standard procedure.

For ChIP, 50 ml of mid-log-phase YPD culture was incubated, pelleted, washed, and resuspended in 1 ml of lysis buffer (50 mM Tris-HCl [pH 7.5], 100 mM NaCl, 1.5 mM $MgCl_2$, 0.0075 NP-40, 100 mM dithiothreitol). After breakage, 5 mg/ml extract was incubated overnight at 4°C with 10 μg of anti-FLAG M2 Clone2 monoclonal antibody (Sigma). Thirty microliters of protein A-Sepharose (10%, wt/vol) was incubated overnight at 4°C in 1× bovine serum albumin–phosphate-buffered saline (PBS). Afterwards, the protein A-Sepharose was pelleted, washed with PBS, incubated with the extract and anti-FLAG antibody for 3 h at 4°C, centrifuged, washed with PBS, and resuspended in 40 μl of Laemmli buffer. Finally, Western immunoblot assays using a 10% acrylamide gel and either anti-FLAG or anti-TAP rabbit polyclonal antibody (Thermo Scientific) were performed.

Microarray analysis. Analysis of microarray data was carried out with DNA-Chip Analyzer (www.dchip.org) (41). Normalization of probe cell files and computation of expression values were performed using the Invariant Set Normalization method and the Model Based method, respectively (41). Genes with expression increased or decreased by more than 1.5-fold with respect to the wild type were selected for further study. GO slim terms (Biological Process) were obtained with the SGD Gene Ontology Slim Mapper (http://www.yeastgenome.org/cgi-bin/GO/goSlimMapper.pl). The search for statistically significant terms in the lists of genes up- and downregulated was performed using Gene Ontology Term Finder (http://www.yeastgenome.org/cgi-bin/GO/goTermFinder.pl). Yeast open reading frame (ORF) sequences were obtained from http://downloads.yeastgenome.org/sequence/genomic_sequence/orf_dna/ (May 2009).

Determination of recombination frequencies. Recombination frequencies were determined as described previously (50), using 12 independent colonies for each strain studied. Yeast strains were grown on SC medium plates (those carrying the intrachromosomal direct-repeat system *leu2-k*::*URA3-ADE2*::*leu2-k*) or on SC medium lacking uracil (SC-ura) (those carrying the plasmid-borne direct-repeat system LYΔNS). After 4 days, independent colonies were picked, resuspended in water, and plated in SC medium containing 5-fluoroorotic acid for the *leu2-k*::*URA3-ADE2*::*leu2-k* system or on SC-ura-leu plates for the LYΔNS system. The number of Ura^- or Leu^+ recombinant colonies was quantified, and the median frequency of recombination of each strain per viable cell number was calculated (determined on SC medium or SC-ura).

Miscellaneous. Northern analyses were performed according to standard procedures with ^{32}P-radiolabeled probes. RNA was isolated from mid-log-phase cells, transformed with either the *tet*::*lacZ-URA3* or the *tet*::*LEU2* system, and grown in SC medium without doxycycline. As a ^{32}P-labeled DNA probe, we used a 3-kb BamHI *lacZ* fragment, a 0.4-kb ClaI-EcoRV *LEU2* fragment, and the internal 589-bp 28S rRNA fragment obtained by PCR (7). For the *MED10* and *SCH9* probes, PCR fragments were obtained from genomic DNA using primers 5′ATGGAAACAGCACTAACAATGA3′and 5′TCAATGGGAGATGTTCTCTTTA3′ (MED10) or 5′ATCGTCGAATCAGGATACTGGA3′ and 5′TTACCGTTGGCATCGAGTAGAA3′ (SCH9).

RNA export was determined by *in situ* localization with digoxigenin-labeled $oligo(dT)_{16}$ (3). Samples were taken from mid-log-phase cultures and shifted to 37° for 4 h. Nuclei (DNA) were visualized by staining with 10 μg/ml 4′,6-diamidino-2-phenylindole (DAPI). Analyses were performed in an Olympus AHBT3 microscope.

RESULTS

A search for suppressors of the gene expression defect of the *hpr1*Δ mutant. To get further insight into mRNP biogenesis and the functional role of the THO complex in gene expression, we searched for new genes that could have a function related to that of THO. For this, we used the centromeric plasmid pCM184-LAUR containing a 4.15-kb *lacZ-URA3* translational fusion under the control of the *tet* promoter. Wild-type cells express this fusion protein, and consequently, they can form colonies on SC-ura. On the contrary, THO mutants, like the *hpr1*Δ mutant, do not express the *lacZ-URA3* fusion at sufficient levels and therefore do not form colonies on SC-ura (35). Using this assay, we searched for new *hpr1*Δ suppressors with the yeast genomic library mutagenized with the mTn*3-lacZ/LEU2* transposon (5). From approximately 22,000 yeast transformants with the insertion library tested, we selected 90 clones that recovered the capacity of *hpr1*Δ mutant cells to grow in SC-ura. After confirming by Northern blotting that pLAUR RNA levels were indeed increased (data not shown) and that the Tn*3* insertion marker (*LEU2*) cosegregated with the suppressor phenotype, genomic DNA from the selected clones was isolated and the DNA around the insertion was sequenced. This allowed us to select three different mutants. In two of them, Tn*3* was inserted in the promoter of the *SCH9* and *MED10* essential genes (*sch9-101* and *med10-101*), respectively. Tn*3* insertion caused a reduction in the expression of both genes (Fig. 1C). The third insertion was in the middle of the ORF of *YPR045c*, a new gene that will be referred to as *THP3* (THO-related protein 3) from now on (*thp3-101*). Figure 1A shows that *hpr1*Δ *thp3-101*, *hpr1*Δ *med10-101*, and *hpr1*Δ *sch9-101* double mutants harboring the pLAUR system recover the capacity to grow in SC-ura. In Fig. 1B, we show that, indeed, there is an increase in mRNA levels of the *lacZ-URA3* fusion in the double mutants compared with that in the *hpr1*Δ simple mutant.

Partial suppression of all *hpr1*Δ phenotypes by mutation of *YPR045c*/*THP3*, *MED10*, and *SCH9*. We assayed next whether suppression of the gene expression defect of *hpr1*Δ mutant cells by *thp3-101*, *med10-101*, and *sch9-101* was general for any phenotype of *hpr1*Δ mutant cells, including mRNA export and recombination or whether it was specific for transcription. RNA export of total $poly(A)^+$ RNA was assayed by *in situ* hybridization with Cy3-conjugated oligo(dT)s. As shown in Fig. 2A, the strong nuclear accumulation of $poly(A)^+$ RNA disappeared from all double mutants. Finally, we determined the ability of the three mutations to suppress the hyperrecombination phenotype of the *hpr1*Δ single mutant. As shown in Fig. 2B, the three mutations were able to reduce the frequency of recombination by 4- to 5-fold. Suppression was not complete for any of the three phenotypes analyzed, but it was clearly general and not specific for a particular phenotype. This sug-

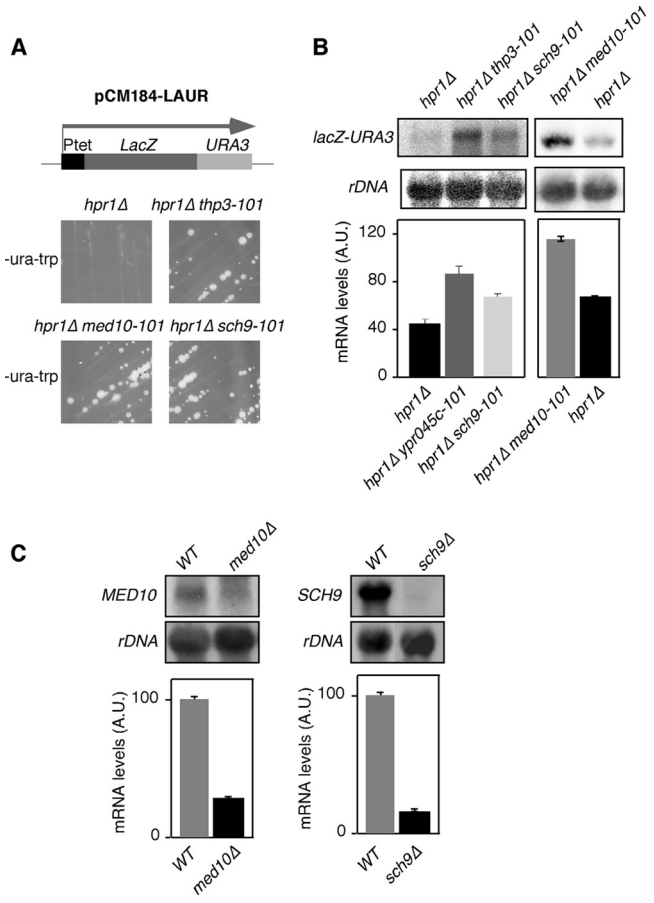

FIG. 1. Suppression of the gene expression phenotype of *hpr1*Δ by the *YPR045c*/*THP3*, *MED10*, and *SCH9* mutations. (A) Phenotypic analysis of *hpr1*Δ (U678-1C), *hpr1*Δ *thp3-101*, *hpr1*Δ *med10-101*, and *hpr1*Δ *sch9-101* isogenic strains transformed with the pLAUR system. The capacity of each strain to form colonies on SC-ura after 4 days at 30°C is shown. A scheme of the pLAUR system is shown at the top. (B) Northern blot analyses of the strains shown in panel A. RNA levels in arbitrary units (A.U.) were obtained in a Fuji FLA 3000 and normalized with respect to the rRNA levels of each sample. (C) Northern analyses of the *MED10* and *SCH9* endogenous genes in the wild-type (*WT*; WA41-6B) and *med10-101* (WA48-4B) and *sch9-101* (WB45-1D) mutant congenic strains. Other details are as in panel B.

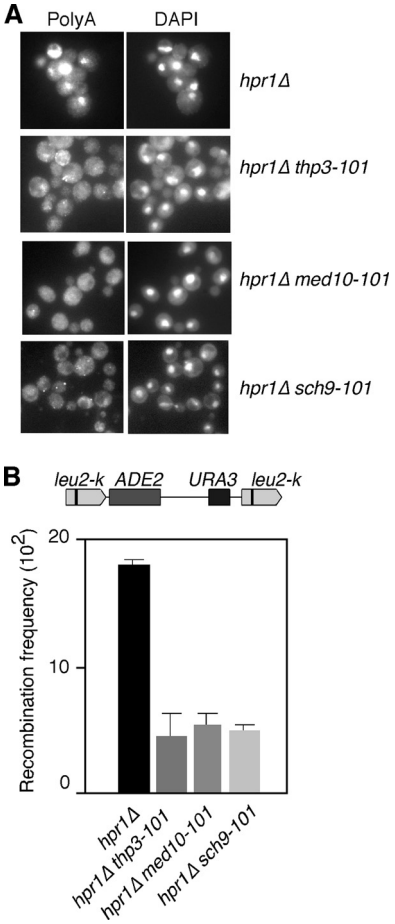

FIG. 2. Suppression of the RNA export and hyperrecombination phenotypes of *hpr1*Δ mutant cells by the *YPR045c*/*THP3*, *MED10*, and *SCH9* mutations. (A) Subcellular localization of poly(A)$^+$ RNAs detected by *in situ* hybridization with digoxigenin-labeled oligo(dT)$_{16}$ of *hpr1*Δ (U678-1C), *hpr1*Δ *thp3-101*, *hpr1*Δ *med10-101*, and *hpr1*Δ *sch9-101* isogenic strains. Samples were taken from mid-log-phase cultures and shifted to 37°C for 4 h. (B) Recombination frequency of the intrachromosomal direct-repeat system *leu2-k*::*URA3-ADE2*::*leu2-k* in *hpr1*Δ (AYW3-3C), *hpr1*Δ *ypr045c-101* (WA41-2B), *hpr1*Δ *med10-101*(WA48-1D), and *hpr1*Δ *sch9-101* (WB45-5B) mutant isogenic strains. A schematic of the recombination assay is shown at the top.

gests that the three mutations suppressed the general effect of THO mutations.

Sch9 is a major target of TORC1 in *S. cerevisiae* (62). It is a kinase involved in regulation of RNAPIII transcription by phosphorylation of the Maf1 repressor (39). Nut2/Med10 is a component of the RNAPII mediator complex (27). The putative function of the *SCH9* and *MED10* genes related to transcription might cause the mutations to reduce the rate of transcription, alleviating the need for the THO complex in mRNP biogenesis (see Discussion). Little is known about Thp3/Ypr045c. It is a nuclear protein with a conserved SAC3 domain, which is also found in the Sac3 component of the THSC complex, but its function is unknown. In high-throughput studies, it has been shown to interact physically with Yra1 and genetically with the Taf9 component of SAGA (37, 47). A recent global analysis of genetic and physical interaction data has shown that Thp3/Ypr045c is also related to Sem1, a factor that interacts with the proteasome and with THSC/TREX-2 (66), but the physiological meaning of this interaction is unknown. For these reasons, we focused all our work on Thp3/Ypr045c.

THP3 mutation specifically suppresses THO complex mutations. We wondered whether the suppression conferred by *thp3-101* was specific for THO mutations or if it was general for mutations in other genes with a role at the transcription-RNA export interface that conferred phenotypes similar to those conferred by THO mutations. We tested the ability of *thp3-101* to suppress *mft1*Δ, a subunit of THO, the *thp1*Δ mutation of the THSC complex, and the *mex67-5* mutation of the Mex67-Mtr2 RNA export factor. As shown in Fig. 3, *thp3-101* was able to suppress the inability of the *mft1*Δ mutant to form colonies in medium lacking uracil and therefore to express *lacZ-URA3* at the appropriate levels to support growth. Instead, this suppression was not observed in *thp1*Δ *thp3-101* and *mex67-5*

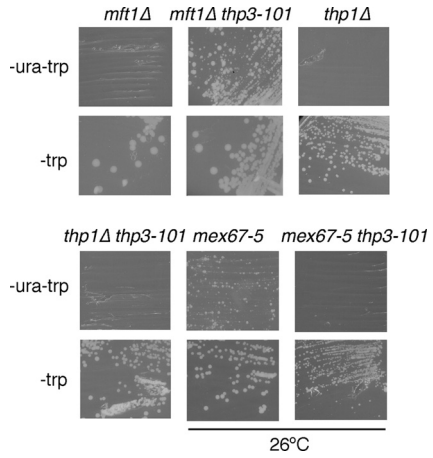

FIG. 3. Specificity of the suppression of the gene expression phenotype of the *hpr1*Δ mutant by the *THP3* mutation. Phenotypic analysis of *mft1*Δ (WMK-1A), *mft1*Δ *thp3-101* (WWM-1D), *mex67-5* (WMC1), *mex67-5 thp3-101* (WMM-12D), *thp1*Δ (WFBE046), and *thp1*Δ *thp3-101* (WMT-2C) mutant strains transformed with the pLAUR system. The capacity of each strain to form colonies on SC-ura after 4 days at 30°C or 26°C is shown. Other details are the same as in Fig. 1A.

thp3-101 double mutants. Actually, the *mex67-5 thp3-101* double mutant is very sick and does not grow at 30°C (Fig. 3). This implies that *thp3-101* specifically suppresses mutations of the THO complex, not only of Hpr1, whereas it does not suppress other mRNP biogenesis- and export-related mutations. Therefore, Thp3 might be a protein with a function related to that of THO.

Transcription is impaired in *thp3*Δ mutants. Given the genetic relationship of the *thp3* mutation with THO mutations, we asked whether this mutation also impairs transcription elongation. We first determined the capability of *thp3-101* mutant cells to transcribe *tetp*::*lacZ-URA3* of the plasmid-borne pLAUR system. As shown in Fig. 4A, *thp3-101* mutants accumulated *lacZ-URA3* RNA at levels below 50% of that of the wild type. However, in the shorter *tetp*::*LEU2* control system, the *LEU2* transcript accumulated at 30% of the wild-type levels (Fig. 4B). This suggests that the *thp3* mutant may have a defect in the activation of the *tet* promoter.

Consequently, we would expect that *thp3-101* may have a general effect in transcription.

Previously, analysis of RNAPII recruitment by ChIP analysis was used to assess *in vivo* transcription impairment in several mutants. ChIPs were performed at the 8-kb-long *YLR454c* gene fused to the *GAL1* promoter in three different regions (5′ end, middle, and 3′ end). In the wild-type strain, above 95% of the RNAPIIs reached the 3′ end of the gene and this value was significantly reduced in mutants defective in transcription elongation, such as *spt4* or *THO* mutants (43). Analysis of the distribution of RNAPII at the *GAL1p*::*YLR454* construct revealed that the relative levels of RNAPII throughout the promoter, 5′, and 3′ regions did not change in wild-type or *thp3-101* mutant cells, but in *thp3-101* mutant cells, the overall levels were half of the wild-type levels at the three positions tested (Fig. 4C). These results indicate a general reduction in transcription but do not offer a clear answer about an effect on transcription elongation. In this sense, it is worth noting that

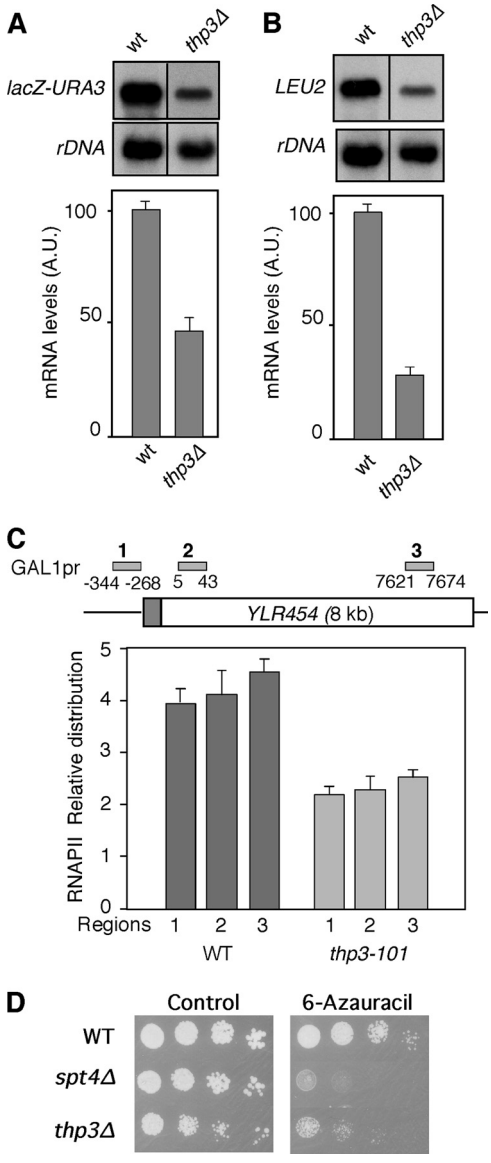

FIG. 4. Transcription analysis of *thp3*Δ mutants. (A) Northern analysis of the *Ptet*::*lacZ-URA3* fusion in the wild-type (wt or WT) and *thp3*Δ mutant (BWMN-2B) congenic strains. Other details are as in Fig. 1B. A.U., arbitrary units. (B) Gene expression analysis of the pCM189-LEU2 construct. Analysis of the capacity of the *thp3*Δ mutant and wild-type strains to transcribe the *Ptet*::*LEU2* construct, measured by Northern blot analysis, is shown. Other details are as in Fig. 1B. (C) RNAPII occupancy at the *GAL1-YLR454w* gene in the *thp3-101* mutant. ChIP analyses (using 8WG16 anti-RNPII antibodies) in the wild-type (W303) and *thp3-101* mutant (WM454-2B) isogenic strains carrying the *GAL1p*::*YLR454w* fusion construct located at the endogenous *YLR454w* chromosomal locus are shown. A schematic of the gene and the PCR-amplified fragments is shown. The DNA ratios in the promoter (bars 1), 5′ (bars 2), and 3′ (bars 3) regions were calculated from the DNA amounts in these regions relative to that in the intergenic region. Medians and SD of three independent experiments are shown. (D) Sensitivity of the *thp3*Δ mutant to 6-azauracil. Tenfold serial dilutions of the wild-type (BY4741) and *thp3*Δ and *spt4*Δ mutant isogenic strains were cultured for 4 days at 30°C in YPD medium either with or without 6-azauracil.

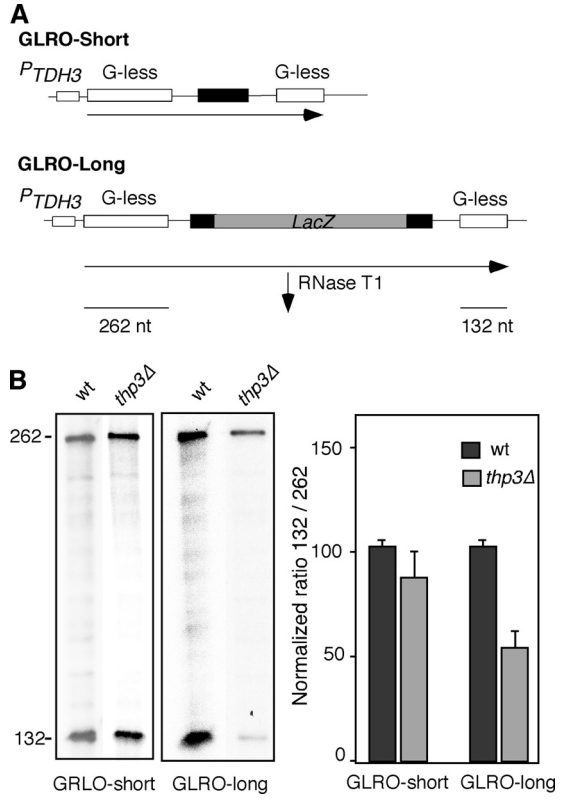

FIG. 5. Effect of *thp3*Δ on transcription elongation. (A) Schematic of tandem G-less cassette constructs pG-leu-CYCds (GLRO-short) and pCYCLacZ (GLRO-long). (B) GLRO analysis of wild-type (wt; BY4741) and *thp3*Δ mutant isogenic strains transformed with pG-leu-CYCds and pCYCLacZ systems. The rectangles represent the two G-less cassettes. Transformants were grown in SC-leu medium to exponential phase and run on transcription assays were performed as described in Materials and Methods. Radioactivity incorporated into the G-less cassettes was quantified in a Fuji FLA-5100. For each sample, the ratio of the total numbers of counts incorporated into the distal versus the proximal G-less cassette was determined and normalized against the ratio for the same construct in the wild-type strain. The average and SD of three independent experiments are shown. The values to the left are molecular sizes in nucleotides.

mutations in the yeast PAF complex show a similar RNAPII ChIP distribution (45). However, this complex has been shown to be required for transcription elongation *in vitro* (57) and *in vivo* (C. Tous et al., unpublished). Similarly, the role of human PAF in transcription elongation has been demonstrated in a chromatin template (36).

Furthermore, we have observed that, as is the case for the *thp3-101* allele obtained in our screening, the *thp3*Δ null mutant is able to suppress the transcriptional defect of the *hpr1*Δ mutant (see Fig. S1 in the supplemental material) and is sensitive to 6-azauracil, an inhibitor of transcription elongation (Fig. 4D).

Finally, we directly assayed the effect of *thp3*Δ on transcription elongation. This was done *in vivo* with a novel assay based on a run-on analysis of transcription units carrying two G-less cassettes (GLRO assays). The GLRO assays are based on two plasmid-borne constructs containing two G-less cassettes of 262 nucleotides (nt) and 132 nt separated by a 243-nt *CYC1* (GLRO-short) or a 2-kb *lacZ* (GLRO-long) fragment as a spacer sequence; both cassettes are under the control of the strong and constitutive *TDH3* promoter (Tous et al., unpublished) (Fig. 5A). Transcription elongation was measured by run-on analysis, followed by purification of synthesized RNAs and subsequent RNase T1 treatment, which does not degrade G-less RNAs. Figure 5B shows that the efficiency of transcription elongation, as assayed by the ability to transcribe the downstream 243-nt G-less cassette versus the upstream 132-nt cassette, was 80% of the wild-type level for the GLRO-short system and 56% of the wild-type level for the GLRO-long system. This result clearly shows that transcription elongation is defective in *thp3*Δ mutant cells, this defect being more evident for long transcripts, consistent with the idea that the longer the transcription unit analyzed the higher the transcription elongation defect expected, even though it does not exclude the possibility that it can also work in initiation.

Thp3 is recruited to ORFs in a transcription-dependent manner. We next asked whether this protein is recruited to transcriptionally active ORFs. For this, we used a wild-type strain containing a TAP-tagged Thp3 protein and determined by quantitative PCR the recruitment of Thp3 to the constitutive *PMA1* gene and the regulated *GAL1* gene, the latter under both repressed (2% glucose) and activated (2% galactose) conditions. As shown in Fig. 6A, Thp3 was clearly recruited to the three regions of *PMA1*, the proximal 5′-end, the middle, and the distal 3′-end regions, with similar amounts in all of the regions. For *GAL1* under repressed conditions, Thp3 recruitment was almost undetectable along the 5′-end, middle, and 3′-end ORF regions, as well as the untranslated region. Instead, under activated transcription conditions, Thp3 was recruited all over the gene from the 5′-end to the 3′-end ORF region (Fig. 6B). Therefore, consistent with its putative role in elongation, Thp3 is recruited to transcribed ORFs.

Thp3 forms a physical and functional complex with Csn12. To get further insight into the function of Thp3, we undertook a biochemical analysis aimed at identifying other proteins that physically interacted with Thp3 *in vivo*. For this, we used a strain carrying a TAP-tagged Thp3 protein to purify *in vivo* Thp3-bound proteins by two-step chromatography purification. After establishing that the protein bands obtained in the purification were specific to the Thp3-TAP strain (Fig. 7A), we identified them by MALDI-TOF. As shown in Fig. 7B, Csn12, which has been shown to interact with the CSN, was clearly copurified with Thp3. In addition to Csn12, we obtained several ribosomal proteins that appeared in the Thp3-TAP but not in the control strain (Fig. 7A and B).

We asked next whether Thp3-Csn12 forms a functional unit and whether or not it functions in the context of the signalosome. For this, we analyzed whether *csn12*Δ suppresses the transcription defect of *hpr1*Δ mutant cells, as was the case for *thp3*Δ, and we compared the results with those of *csn9*Δ, a *bona fide* representative of the signalosome complex and the related *sem1*Δ mutant. Indeed, *csn12*Δ, but not *csn9*Δ or *sem1*Δ, was able to suppress the thermosensitivity of *hpr1*Δ, as well as its inability to transcribe the *lacZ-URA3* ORF, as determined by the capacity to grow on SC-ura (Fig. 8A). We have also checked that the *csn12*Δ mutation, as is the case for *thp3*Δ, partially suppresses the hyperrecombination phenotype due to *hpr1*Δ, as determined with the LYΔNS plasmid-borne recombination system (Fig. 8B). Therefore, suppression of THO

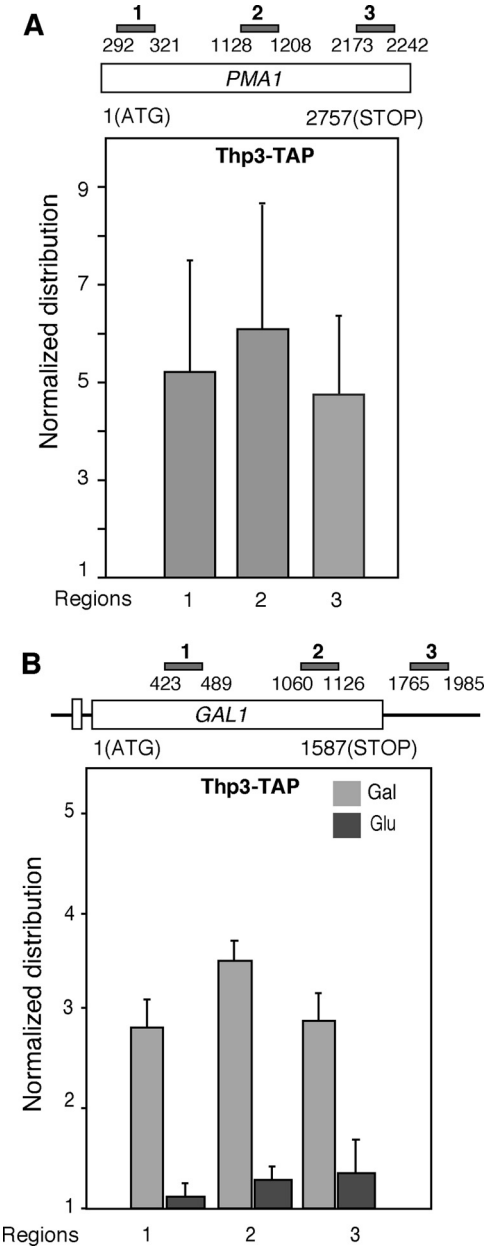

FIG. 6. Recruitment of Thp3-TAP to transcribed chromatin. (A) ChIP analysis of Thp3 at the endogenous *PMA1* gene in the wild-type strain carrying TAP-tagged Thp3 (from Open Biosystems). A schematic of the gene analyzed and the amplified PCR fragments is shown. The median and SD of three independent experiments are shown. (B) ChIP analysis of Thp3 at the endogenous *GAL1* gene. Other details are as in panel A.

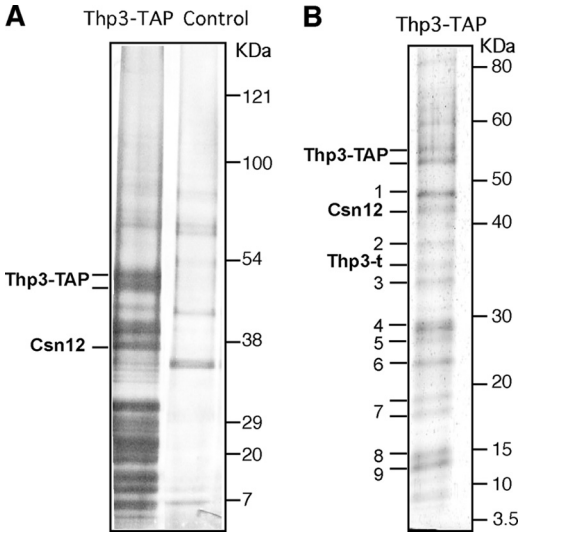

FIG. 7. Purification of a Thp3 protein complex. (A) TAP and its blank control. Isogenic (BY4741) Thp3-TAP and untagged strains were used for TAP. A 4 to 12% gradient gel (NuPAGE Novex Bis-Tris from Invitrogen) and silver stain were used. (B) Thp3-TAP proteome. Silver-stained 8 to 16% gradient SDS-PAGE of the Thp3-TAP-tagged complex purified from wild-type cells. In addition to the full Thp3 and Csn12 proteins, we obtained truncated Thp3 (Thp3-t); ribosomal proteins Rpl3 (band 1), Rpl4 (bands 2 and 4), Rpl7 (band 6), Rps13 (band 8), and Rps16 (band 9); and the common TAP contaminants Tdh3 (band 3), Eef2 (calmodulin-dependent protein) (band 5), and human calpain (band 7).

mutations is specifically shared by *thp3*Δ and *csn12*Δ and not by mutations in the signalosome complex. In agreement with this conclusion, we have observed that *thp3*Δ and *csn12*Δ confer sensitivity to mycophenolic acid (MPA), a drug that depletes cells of GTP, impairing transcription elongation (28), whereas this is not the case for *csn9*Δ (Fig. 8C). We have further confirmed by coimmunoprecipitation analyses that the interaction between Thp3 and Csn12 is specific and not shared by other components of the signalosome. As shown in Fig. 9, Thp3 coprecipitated with Csn12 but not with Csn9. Moreover, Northern analysis of transcription of *csn12*Δ mutant cells revealed that they yield about 75% of the total *lacZ-URA3* transcripts from the pLAUR system, implying a defect in transcription, although weaker than that of *thp3*Δ mutant cells in this assay (Fig. 10A). However, in the shorter *tetp*::*LEU2* control system, the *LEU2* transcript accumulated at the same levels as in the wild type (Fig. 10B), implying that *thp3*Δ did not have a negative effect on the activation of the *tet* promoter. Finally, to further confirm that Csn12 was not only physically but functionally related to Thp3, we determined the ability of a TAP-tagged Csn12 protein to immunoprecipitate chromatin. As shown in Fig. 10C, Csn12 was recruited throughout the *PMA1* gene at the three positions tested, the 5′ end, the middle, and the 3′ end. Furthermore, using the inducible *GAL1* endogenous gene, we have seen that, as is the case for Thp3, Csn12 is recruited to transcribed chromatin. Recruitment to *GAL1* was detected only in galactose-containing medium (Fig. 10D). We can therefore conclude that Csn12 and Thp3 form a physical and functional unit with a role in transcription. Our results therefore confirm a role for Thp3-Csn12 in transcription elongation *in vivo* that is functionally independent of the signalosome.

To know whether the presence of a number of ribosome proteins in the Thp3-TAP has an additional biological meaning requires a more elaborate analysis. Nevertheless, the fact that ribosomal proteins were not observed in our blank control opens the possibility that Thp3-Csn12 physically interacts with a ribosomal counterpart. Determination of whether or not this implies an additional posttranscriptional function for Thp3-

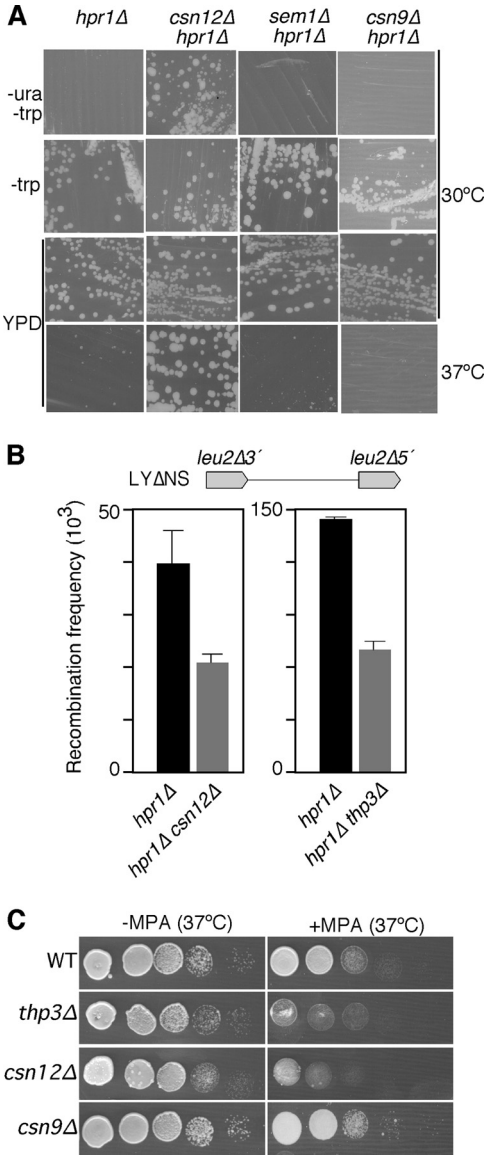

FIG. 8. Genetic analysis of the Thp3 protein complex. (A) Growth on SC-ura of *hpr1*Δ *thp3*Δ (BWMH-8D), *hpr1*Δ *csn12*Δ (BWCH-1B), *hpr1*Δ *sem1*Δ (WSH-2A), and *hpr1*Δ *csn9*Δ (BWC9H-4A) mutant congenic strains carrying the pLAUR system and growth of the same strains in YPD at 30 and 37°C. Other details are as in Fig. 1A. (B) Suppression of the hyperrecombination phenotype of the *hpr1*Δ mutant by the *thp3* and *csn12* mutations. The recombination frequencies of the plasmid-borne direct-repeat system LYΔNS in the *hpr1*Δ (BWMN-2A), *hpr1*Δ *thp3*Δ (BWMN-3B), and *hpr1*Δ *csn12*Δ (WCSHP-3B) mutant congenic strains are shown. A schematic of the recombination assay is shown at the top. (C) Serial dilutions of the wild-type (WT; BY4741) and *thp3*Δ, *csn12*Δ, and *csn9*Δ mutant isogenic strains cultured in YPD medium with and without MPA (150 μg/ml) at 37°C.

Csn12, such as translation or ribosome biosynthesis, requires further investigation.

Genome-wide analysis of gene expression in *thp3*Δ mutants. To assay if the effect of *thp3*Δ was due to the downregulation of a transcription elongation factor, we determined the transcript levels of the whole genome in *thp3*Δ mutant cells by microarray gene expression analysis. Using the Affymetrix platform, we determined the RNA levels of 5,800 genes. Among these, 76 were significantly downregulated (levels ≤0.5 times that of the wild type) (see Table S1 in the supplemental material). They do not share any structural or functional features, and none of them has been shown to have a role in transcription elongation. Therefore, the effect of *thp3*Δ on transcription does not seem to be mediated by a second gene.

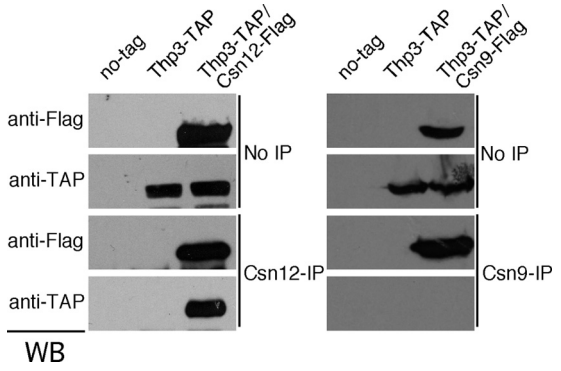

FIG. 9. Specificity of the interaction between Thp3 and Csn12. Experiments in which Thp3-TAP was coimmunoprecipitated with Csn12-FLAG (left) or Csn9-FLAG (right) are shown. Isogenic strains with no tag (BY4741) or carrying both the Thp3-TAP fusion protein and either the Csn12-FLAG (THT-12FLAG) or the Csn9-FLAG (THT-9FLAG) fusion protein were used. IP, immunoprecipitate; WB, Western blotting.

Interestingly, a comparative analysis with previous data for the *thp1*Δ and *tho2*Δ mutants (44) revealed that 28 genes downregulated in the *thp3*Δ mutant are downregulated in the *tho2*Δ mutant and that 30 genes downregulated in the *thp3*Δ mutant are downregulated in the *tho2*Δ mutant. Moreover, 26 of these genes are the same in the three mutants. Interestingly, most of these 26 genes are either subcentromeric (14 out of 26) or subtelomeric (10 out of 26) (see Table S2 and Fig. S2 in the supplemental material). This suggests an intriguing link between Thp3-Csn12 and heterochromatin-proximal regions that would require further analysis to evaluate its biological significance.

DISCUSSION

A search for suppressors of the gene expression defect of the *hpr1*Δ mutant has led to the isolation of insertion mutations in *YPR045c*, *MED10*, and *SCH9*. Previous screenings for suppressors of the *hpr1*Δ mutation have identified several factors involved in transcription. Thus, mutations in components of the mediator of RNAPII like Hrs1/Med3, Srb2/Med20, Gal11/Med15, and Sin4/Med16 have been shown to suppress *hpr1*Δ hyperrecombination (14, 51, 52, 58). Besides, mutations in the Rad3 component of the TFIIH initiation factor suppress the accumulation of transcripts at the site of transcription in *mft1*Δ mutants (33), and the *soh* alleles of Med31, Rpb2, and TFIIB suppress the *hpr1*Δ mutant thermosensitivity phenotype (14). Our identification of Med10 as a suppressor of *hpr1*Δ constitutes new evidence that a defective mediator or RNAPII protein suppresses THO mutations. Interestingly, Soh1/Med31 has been shown to interact with Nut2/Med10 by two-hybrid assay and affinity capture (10). This could imply that a subset of

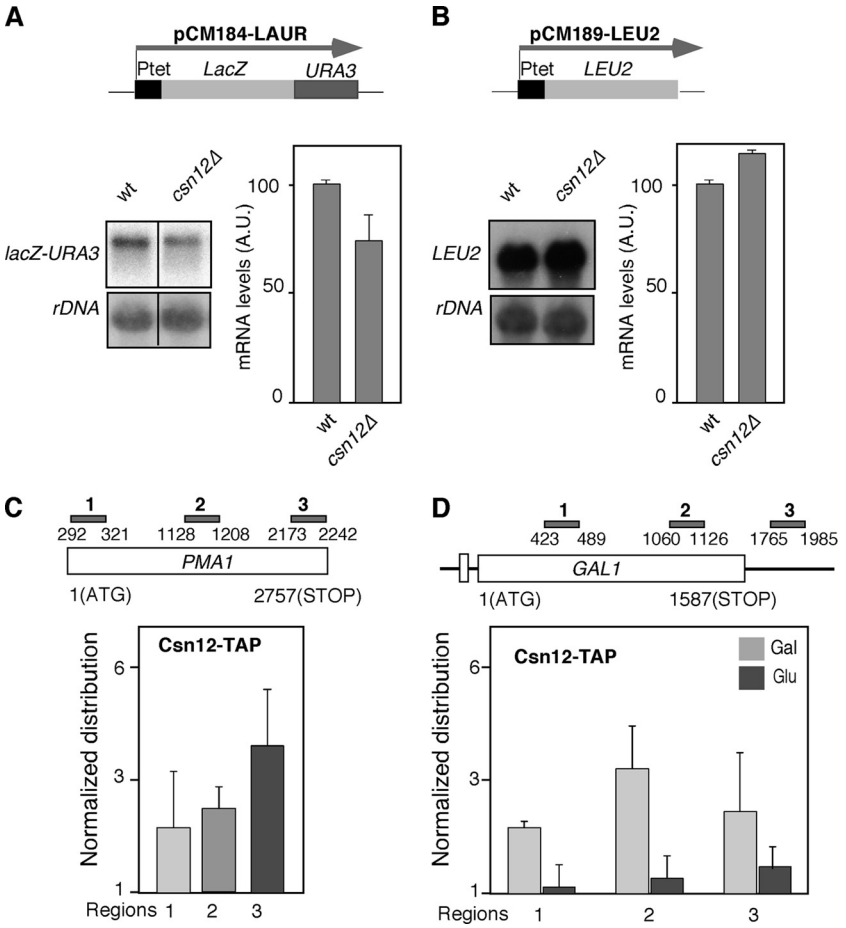

FIG. 10. Characterization of Csn12. (A) Northern analysis of the *lacZ-URA3* fusion in wild-type (wt; BWMN-1A) and *csn12*Δ mutant (BWCS12-3B) congenic strains. Other details are as in Fig. 1B. A.U., arbitrary units. (B) Northern analysis of the *tetp*::*LEU2* fusion. Other details are as in panel A. (C) ChIP analysis of TAP-tagged Csn12 at the *PMA1* gene. (D) ChIP of Csn12-TAP at the *GAL1* gene. Other details are as in Fig. 6.

mediator or RNAPII proteins may functionally interact with THO. However, it seems likely that the common behavior of these suppressors, including *med10*, is a reduction in transcription firing or transcription efficiency, consistent with the observation that a decrease in the strength of transcription can alleviate *hpr1*Δ gene expression defects (33, 34).

The second suppressor isolated in this study is Sch9, a major target of TORC1 in *S. cerevisiae* (62). It is a kinase involved in the regulation of RNAPIII-mediated transcription (39). Interestingly, *SCH9* mutations have also been shown to suppress other transcription-associated recombination events in yeast, as is the case for HOT1-stimulated recombination and ribosomal DNA recombination (53). *SCH9* mutations also suppress the genomic instability of null mutants of the Sgs1 DNA helicase involved in double-strand break repair (43). These results suggest that Sch9 could play a novel role in the control of genomic integrity, but the molecular basis and biological significance of this putative role remain to be seen. Interestingly, different types of genetic interactions have been reported for *SCH9* with *SEM1* and *SOH1*/*MED31* (18) and with *MED10* (59). Sem1 physically interacts with the THSC complex, and its mutation shows defects similar to those observed in THO and THSC complex mutants (15, 66). Altogether, these data may indicate that Sch9, Nut2/Med10, and Soh1/Med31 act in the same genetic pathway, the absence of which alleviates the phenotypes of THO mutants, presumably by altering transcription and mRNP biogenesis to levels that tolerate the absence of THO, as has been suggested for other suppressors (33, 34).

Notably, our suppressor analysis has identified Ypr045c (Thp3). Little is known about this protein. It is nuclear, and it has been previously shown to coimmunoprecipitate with Csn12 together with other proteins, including the Yra1 mRNA export factor (37). We show here that Thp3 has a role in transcription. However, the defect of the *thp3* mutant is not similar to that of *THO* mutants. This is not surprising, given that mutations in the mediator and other transcription factors that also suppress *hpr1* mutations do not have the same function or effect as THO (14, 51, 58). *thp3* mutants have a defect in transcription at both the initiation and elongation steps. The recruitment of Thp3 throughout the whole ORF under active transcription conditions suggests an active role for Thp3 during transcription elongation, although it does not eliminate the possibility of a role in other transcription steps. This active role is confirmed by the sensitivity to 6-azauracil and with the transcription elon-

gation defect that the *thp3*Δ mutant shows in the novel GLRO *in vivo* assay reported here. Besides, we show by genome-wide microarray gene expression analysis that 76 genes show a significant reduction in the steady-state levels of RNA accumulation in the *thp3*Δ mutant. This reduction may be due not only to a decrease in elongation efficiency but likely also to a negative effect on the activation of some promoters, although it cannot be established whether or not this effect is due to a direct role of Thp3-Csn12. Twenty-six of the genes that are downregulated in the *thp3*Δ mutant are also downregulated in THO and THSC mutants, and 24 of these are located in either subtelomeric or subcentromeric regions. Interestingly, it has recently been shown that *src1*Δ, which interacts genetically with THO mutations, is also defective in the expression of subtelomeric genes (26). This opens the possibility that the chromatin structure or nuclear localization of subtelomeric genes makes the expression of such genes particularly dependent on transcription factors such as Thp3-Csn12, THO, and THSC.

Although it has been shown that Ypr045c/Thp3 interacts physically with many factors, including Yra1 and Sem1 (15, 37), purification of a protein complex containing only Ypr045c/Thp3 and Csn12 has not been reported. Csn12 was previously described as part of the CSN. Csn12, like Thp3, coimmunoprecipitates with Sem1, which also interacts with the proteasome and the THSC/TREX-2 complex (15, 66). We did not obtain either Sem1 or any component of the previously mentioned complexes, implying that Thp3 and Csn12 may form an independent core complex *in vivo*. Despite the relationship between Csn12 and the signalosome (46), we did not see a physical interaction with any CSN component in our TAP. Moreover, Thp3 coimmunoprecipitated with Csn12 and not with CSN component Csn9. This, together with the fact that *csn12*Δ suppresses different phenotypes of *hpr1*Δ mutant cells and shows a defect in gene expression while this is not the case for *csn9*Δ, suggests that Thp3 and Csn12 form an independent functional unit with a role in transcription. Besides, as is the case for Thp3, recruitment of Csn12 throughout the whole ORF under active transcription conditions is consistent with a role in transcription.

It is interesting that, in addition to Csn12, we also obtained the ribosomal proteins Rpl3, Rpl4, Rpl7, Rps13, and Rps16 by Thp3-TAP. Actually, there are more data that might indicate some sort of relationship between the Thp3-Csn12 complex and ribosome biogenesis. Thus, it has been shown that Thp3 interacts physically with Ebp2, Rpf2, and Rrs1 (37), the three of them being implicated in preribosomal 60S particle assembly. Besides, genetic interactions between *thp3* and *rps16* mutants and between *csn12* and *rpl37* and *rpso* mutants have also been shown (11). Altogether, these data indicate that the physical interaction between the Thp3-Csn12 complex and the ribosomal proteins may imply a functional interconnection between Thp3-Csn12 and ribosome biogenesis or translation that requires further analysis. In this sense, it is worth noting that it has recently been shown that the yeast RNAPII holoenzyme subunits Rpb4 and Rpb7 shuttle between the nucleus and the cytoplasm, functioning in both transcription and translation (29). Besides, it is interesting that several ribosomal proteins, including L7, S13, and S16, found in our TAPs can be modified by NEDD8 (67), which opens the possibility of an interaction between Thp3-Csn12 and the CSN. In this sense, a more detailed study is required to determine to what degree Thp3-Csn12 might also be involved in ribosomal biogenesis and metabolism, apart from or in relation to its role in transcription elongation shown here.

Recently, it has been suggested that *CSN12* and *YPR045c*/*THP3* may be involved in splicing, based on the profile of genetic interactions of *csn12*Δ and on the splicing-specific microarray gene expression patterns of mutants affected in both genes (66). Our work further supports a role for these proteins in RNA metabolism. Nevertheless, as all of our observations are based on intronless genes, we conclude that the role of Thp3 in transcription elongation that we describe here is independent of splicing.

Different studies have provided indications for a putative relationship between the CSN and gene expression. Thus, it was originally described as a transcriptional repressor of a range of *Arabidopsis* genes (13, 16, 64), and mutations of different subunits of the CSN in *Drosophila* leads to misregulation of 20% of the transcriptome during larval development (49). The molecular basis of this relationship, whether direct or indirect, is unclear (for a review, see reference 6).

Interestingly, the Thp3-Csn12 complex has in common with THSC and the 26S proteasome the presence of one subunit with a Sac3 domain and another subunit with a PAM domain (8, 15, 66). In addition to the known connection of THSC with transcription elongation and mRNP biogenesis (24), different studies have also related the proteasome to transcription. Thus, the 19S regulatory particle of the proteasome has been shown to have a role in transcription elongation (17), and its components are recruited to the entire ORF of transcribed genes (23). As with THSC (56) and Thp3 (47), a genetic interaction between SAGA and the proteasome has been reported (38). Altogether, these results support a role for Thp3-Csn12 in transcription elongation at the interface with mRNA processing.

Using ChIP, we have ruled out the possibility that the chromatin recruitment of THO is dependent on Thp3 and vice versa (Fig.S3). However, the role of Thp3 in transcription may provide a simple explanation for the suppression of the transcriptional phenotype of THO mutants. As discussed above for other *hpr1*Δ suppressors, suppression could be due to a reduction in the transcription rate. However, there are several reasons to believe that this might not be the case. Previously identified mutations that suppress *hpr1*Δ on the basis of reducing transcription also suppresses the *thp1*Δ mutation of the THSC complex (22), whereas *thp3*Δ only suppresses THO mutations. Also, the physical interaction of Thp3 with the Yra1 and Sem1 proteins involved in RNA export (15, 19), the genetic interaction that we observed between *thp3-101* and *mex67-5* (Fig. 3), and the observation that the group of genes downregulated in *thp3*Δ, *thp1*Δ, and *tho2*Δ mutant cells is enriched in subtelomeric genes, similar to RNA processing protein Src1 mutants, suggest a functional interaction of Thp3-Csn12 with mRNP biogenesis and export that is not observed for general transcription factors. Further analysis is required to understand the mechanism of the suppression of THO mutants by Thp3-Csn12 mutations and to establish the precise role of Thp3-Csn12 in transcription at both the initiation and elongations steps, its connection to mRNP biogenesis, and whether or

not this role is related to the CSN. Our study, however, opens new perspectives on our understanding of the connection of transcription with mRNP biogenesis and export.

ACKNOWLEDGMENTS

We thank D. Brow for plasmids, R. Luna and A. Rondón for critical reading of the manuscript, S. Juarez and S. Ciordia from the Proteomic Unit of CNB for the MALDI-TOF identification of the Thp3 proteome, and D. Haun for style supervision.

This work was supported by grants from the Spanish Ministry of Science and Education (BFU2006-05260 and BFU2007-28647-E) and Junta de Andalucía (BIO102 and CVI2549). S.J. was the recipient of a Juan de la Cierva grant from the Spanish Ministry of Science and Innovation. M.R. was funded by Koningin Wilhelmina Fonds and Stichting Nijmegen Universiteits Fonds.

REFERENCES

1. **Aguilera, A.** 2005. Cotranscriptional mRNP assembly: from the DNA to the nuclear pore. Curr. Opin. Cell Biol. **17:**242–250.
2. **Aguilera, A., and B. Gomez-Gonzalez.** 2008. Genome instability: a mechanistic view of its causes and consequences. Nat. Rev. Genet. **9:**204–217.
3. **Amberg, D. C., A. L. Goldstein, and C. N. Cole.** 1992. Isolation and characterization of RAT1: an essential gene of *Saccharomyces cerevisiae* required for the efficient nucleocytoplasmic trafficking of mRNA. Genes Dev. **6:**1173–1189.
4. **Buratowski, S.** 2005. Connections between mRNA 3′ end processing and transcription termination. Curr. Opin. Cell Biol. **17:**257–261.
5. **Burns, N., et al.** 1994. Large-scale analysis of gene expression, protein localization, and gene disruption in *Saccharomyces cerevisiae*. Genes Dev. **8:**1087–1105.
6. **Chamovitz, D. A.** 2009. Revisiting the COP9 signalosome as a transcriptional regulator. EMBO Rep. **10:**352–358.
7. **Chávez, S., et al.** 2000. A protein complex containing Tho2, Hpr1, Mft1 and a novel protein, Thp2, connects transcription elongation with mitotic recombination in *Saccharomyces cerevisiae*. EMBO J. **19:**5824–5834.
8. **Ciccarelli, F. D., E. Izaurralde, and P. Bork.** 2003. The PAM domain, a multi-protein complex-associated module with an all-alpha-helix fold. BMC Bioinformatics **4:**64.
9. **Cole, C. N., and J. J. Scarcelli.** 2006. Transport of messenger RNA from the nucleus to the cytoplasm. Curr. Opin. Cell Biol. **18:**299–306.
10. **Collins, S. R., et al.** 2007. Toward a comprehensive atlas of the physical interactome of *Saccharomyces cerevisiae*. Mol. Cell. Proteomics **6:**439–450.
11. **Costanzo, M., et al.** 2010. The genetic landscape of a cell. Science **327:**425–431.
12. **De Antoni, A., and D. Gallwitz.** 2000. A novel multi-purpose cassette for repeated integrative epitope tagging of genes in *Saccharomyces cerevisiae*. Gene **246:**179–185.
13. **Dohmann, E. M., M. P. Levesque, E. Isono, M. Schmid, and C. Schwechheimer.** 2008. Auxin responses in mutants of the *Arabidopsis* CONSTITUTIVE PHOTOMORPHOGENIC9 signalosome. Plant Physiol. **147:**1369–1379.
14. **Fan, H. Y., and H. L. Klein.** 1994. Characterization of mutations that suppress the temperature-sensitive growth of the hpr1 delta mutant of Saccharomyces cerevisiae. Genetics **137:**945–956.
15. **Faza, M. B., et al.** 2009. Sem1 is a functional component of the nuclear pore complex-associated messenger RNA export machinery. J. Cell Biol. **184:**833–846.
16. **Feng, S., et al.** 2003. The COP9 signalosome interacts physically with SCF COI1 and modulates jasmonate responses. Plant Cell **15:**1083–1094.
17. **Ferdous, A., F. Gonzalez, L. Sun, T. Kodadek, and S. A. Johnston.** 2001. The 19S regulatory particle of the proteasome is required for efficient transcription elongation by RNA polymerase II. Mol. Cell **7:**981–991.
18. **Fiedler, D., et al.** 2009. Functional organization of the S. cerevisiae phosphorylation network. Cell **136:**952–963.
19. **Fischer, T., et al.** 2002. The mRNA export machinery requires the novel Sac3p-Thp1p complex to dock at the nucleoplasmic entrance of the nuclear pores. EMBO J. **21:**5843–5852.
20. **Freilich, S., et al.** 1999. The COP9 signalosome is essential for development of *Drosophila melanogaster*. Curr. Biol. **9:**1187–1190.
21. **Funakoshi, M., X. Li, I. Velichutina, M. Hochstrasser, and H. Kobayashi.** 2004. Sem1, the yeast ortholog of a human BRCA2-binding protein, is a component of the proteasome regulatory particle that enhances proteasome stability. J. Cell Sci. **117:**6447–6454.
22. **Gallardo, M., and A. Aguilera.** 2001. A new hyperrecombination mutation identifies a novel yeast gene, THP1, connecting transcription elongation with mitotic recombination. Genetics **157:**79–89.
23. **Gonzalez, F., A. Delahodde, T. Kodadek, and S. A. Johnston.** 2002. Recruitment of a 19S proteasome subcomplex to an activated promoter. Science **296:**548–550.
24. **González-Aguilera, C., et al.** 2008. The THP1-SAC3-SUS1-CDC31 complex works in transcription elongation-mRNA export preventing RNA-mediated genome instability. Mol. Biol. Cell **19:**4310–4318.
25. **González-Barrera, S., M. Garcia-Rubio, and A. Aguilera.** 2002. Transcription and double-strand breaks induce similar mitotic recombination events in Saccharomyces cerevisiae. Genetics **162:**603–614.
26. **Grund, S. E., et al.** 2008. The inner nuclear membrane protein Src1 associates with subtelomeric genes and alters their regulated gene expression. J. Cell Biol. **182:**897–910.
27. **Gustafsson, C. M., et al.** 1998. Identification of new mediator subunits in the RNA polymerase II holoenzyme from *Saccharomyces cerevisiae*. J. Biol. Chem. **273:**30851–30854.
28. **Hampsey, M.** 1997. A review of phenotypes in *Saccharomyces cerevisiae*. Yeast **13:**1099–1133.
29. **Harel-Sharvit, L., et al.** 2010. RNA polymerase II subunits link transcription and mRNA decay to translation. Cell **143:**552–563.
30. **Hecht, A., and M. Grunstein.** 1999. Mapping DNA interaction sites of chromosomal proteins using immunoprecipitation and polymerase chain reaction. Methods Enzymol. **304:**399–414.
31. **Huertas, P., and A. Aguilera.** 2003. Cotranscriptionally formed DNA:RNA hybrids mediate transcription elongation impairment and transcription-associated recombination. Mol. Cell **12:**711–721.
32. **Huertas, P., M. L. Garcia-Rubio, R. E. Wellinger, R. Luna, and A. Aguilera.** 2006. An *hpr1* point mutation that impairs transcription and mRNP biogenesis without increasing recombination. Mol. Cell. Biol. **26:**7451–7465.
33. **Jensen, T. H., et al.** 2004. Modulation of transcription affects mRNP quality. Mol. Cell **16:**235–244.
34. **Jimeno, S., M. Garcia-Rubio, R. Luna, and A. Aguilera.** 2008. A reduction in RNA polymerase II initiation rate suppresses hyper-recombination and transcription-elongation impairment of THO mutants. Mol. Genet. Genomics **280:**327–336.
35. **Jimeno, S., A. G. Rondón, R. Luna, and A. Aguilera.** 2002. The yeast THO complex and mRNA export factors link RNA metabolism with transcription and genome instability. EMBO J. **21:**3526–3535.
36. **Kim, J., M. Guermah, and R. G. Roeder.** 2010. The human PAF1 complex acts in chromatin transcription elongation both independently and cooperatively with SII/TFIIS. Cell **140:**491–503.
37. **Krogan, N. J., et al.** 2006. Global landscape of protein complexes in the yeast Saccharomyces cerevisiae. Nature **440:**637–643.
38. **Lee, D., et al.** 2005. The proteasome regulatory particle alters the SAGA coactivator to enhance its interactions with transcriptional activators. Cell **123:**423–436.
39. **Lee, J., R. D. Moir, and I. M. Willis.** 2009. Regulation of RNA polymerase III transcription involves SCH9-dependent and SCH9-independent branches of the target of rapamycin (TOR) pathway. J. Biol. Chem. **284:**12604–12608.
40. **Lei, E. P., et al.** 2003. Sac3 is an mRNA export factor that localizes to cytoplasmic fibrils of nuclear pore complex. Mol. Biol. Cell **14:**836–847.
41. **Li, C., and W. H. Wong.** 2001. Model-based analysis of oligonucleotide arrays: expression index computation and outlier detection. Proc. Natl. Acad. Sci. U. S. A. **98:**31–36.
42. **Luna, R., H. Gaillard, C. González-Aguilera, and A. Aguilera.** 2008. Biogenesis of mRNPs: integrating different processes in the eukaryotic nucleus. Chromosoma **117:**319–331.
43. **Madia, F., et al.** 2008. Longevity mutation in *SCH9* prevents recombination errors and premature genomic instability in a Werner/Bloom model system. J. Cell Biol. **180:**67–81.
44. **Marín, A., et al.** 2003. Relationship between G+C content, ORF-length and mRNA concentration in *Saccharomyces cerevisiae*. Yeast **20:**703–711.
45. **Mason, P. B., and K. Struhl.** 2005. Distinction and relationship between elongation rate and processivity of RNA polymerase II *in vivo*. Mol. Cell **17:**831–840.
46. **Maytal-Kivity, V., E. Pick, R. Piran, K. Hofmann, and M. H. Glickman.** 2003. The COP9 signalosome-like complex in *S. cerevisiae* and links to other PCI complexes. Int. J. Biochem. Cell Biol. **35:**706–715.
47. **Milgrom, E., R. W. West, Jr., C. Gao, and W. C. Shen.** 2005. TFIID and Spt-Ada-Gcn5-acetyltransferase functions probed by genome-wide synthetic genetic array analysis using a *Saccharomyces cerevisiae* taf9-ts allele. Genetics **171:**959–973.
48. **Mundt, K. E., et al.** 1999. The COP9/signalosome complex is conserved in fission yeast and has a role in S phase. Curr. Biol. **9:**1427–1430.
49. **Oron, E., et al.** 2007. Genomic analysis of COP9 signalosome function in *Drosophila melanogaster* reveals a role in temporal regulation of gene expression. Mol. Syst. Biol. **3:**108.
50. **Piruat, J. I., and A. Aguilera.** 1998. A novel yeast gene, THO2, is involved in RNA pol II transcription and provides new evidence for transcriptional elongation-associated recombination. EMBO J. **17:**4859–4872.
51. **Piruat, J. I., and A. Aguilera.** 1996. Mutations in the yeast *SRB2* general transcription factor suppress hpr1-induced recombination and show defects in DNA repair. Genetics **143:**1533–1542.
52. **Piruat, J. I., S. Chávez, and A. Aguilera.** 1997. The yeast *HRS1* gene is involved in positive and negative regulation of transcription and shows genetic characteristics similar to *SIN4* and *GAL11*. Genetics **147:**1585–1594.

53. **Prusty, R., and R. L. Keil.** 2004. *SCH9*, a putative protein kinase from Saccharomyces cerevisiae, affects HOT1-stimulated recombination. Mol. Genet. Genomics **272:**264–274.
54. **Rabut, G., and M. Peter.** 2008. Function and regulation of protein neddylation. 'Protein modifications: beyond the usual suspects' review series. EMBO Rep. **9:**969–976.
55. **Rigaut, G., et al.** 1999. A generic protein purification method for protein complex characterization and proteome exploration. Nat. Biotechnol. **17:** 1030–1032.
56. **Rodríguez-Navarro, S., et al.** 2004. Sus1, a functional component of the SAGA histone acetylase complex and the nuclear pore-associated mRNA export machinery. Cell **116:**75–86.
57. **Rondón, A. G., M. Gallardo, M. Garcia-Rubio, and A. Aguilera.** 2004. Molecular evidence indicating that the yeast PAF complex is required for transcription elongation. EMBO Rep. **5:**47–53.
58. **Santos-Rosa, H., and A. Aguilera.** 1995. Isolation and genetic analysis of extragenic suppressors of the hyper-deletion phenotype of the *Saccharomyces cerevisiae hpr1* delta mutation. Genetics **139:**57–66.
59. **Scholes, D. T., M. Banerjee, B. Bowen, and M. J. Curcio.** 2001. Multiple regulators of Ty1 transposition in *Saccharomyces cerevisiae* have conserved roles in genome maintenance. Genetics **159:**1449–1465.
60. **Steinmetz, E. J., and D. A. Brow.** 2003. Ssu72 protein mediates both poly(A)-coupled and poly(A)-independent termination of RNA polymerase II transcription. Mol. Cell. Biol. **23:**6339–6349.
61. **Strässer, K., et al.** 2002. TREX is a conserved complex coupling transcription with messenger RNA export. Nature **417:**304–308.
62. **Urban, J., et al.** 2007. Sch9 is a major target of TORC1 in *Saccharomyces cerevisiae*. Mol. Cell **26:**663–674.
63. **Wei, N., D. A. Chamovitz, and X. W. Deng.** 1994. Arabidopsis COP9 is a component of a novel signaling complex mediating light control of development. Cell **78:**117–124.
64. **Wei, N., and X. W. Deng.** 1992. COP9: a new genetic locus involved in light-regulated development and gene expression in Arabidopsis. Plant Cell **4:**1507–1518.
65. **Wei, N., et al.** 1998. The COP9 complex is conserved between plants and mammals and is related to the 26S proteasome regulatory complex. Curr. Biol. **8:**919–922.
66. **Wilmes, G. M., et al.** 2008. A genetic interaction map of RNA-processing factors reveals links between Sem1/Dss1-containing complexes and mRNA export and splicing. Mol. Cell **32:**735–746.
67. **Xirodimas, D. P., et al.** 2008. Ribosomal proteins are targets for the NEDD8 pathway. EMBO Rep. **9:**280–286.
68. **Zhao, Y., et al.** 2008. A TFTC/STAGA module mediates histone H2A and H2B deubiquitination, coactivates nuclear receptors, and counteracts heterochromatin silencing. Mol. Cell **29:**92–101.